Enhancing cellular uptake of GFP via unfolded supercharged protein tags

Pesce, Diego; Wu, Yuzhou; Kolbe, Anke; Weil, Tanja; Herrmann, Andreas

Published in:
Biomaterials

DOI:
10.1016/j.biomaterials.2013.02.038

Publication date:
2013

Biomaterials 34 (2013) 4360–4367

Contents lists available at SciVerse ScienceDirect

Biomaterials

journal homepage: www.elsevier.com/locate/biomaterials

Enhancing cellular uptake of GFP *via* unfolded supercharged protein tags

Diego Pesce [a,1], Yuzhou Wu [b,1], Anke Kolbe [a], Tanja Weil [b,*], Andreas Herrmann [a,*]

[a] Department of Polymer Chemistry, Zernike Institute for Advanced Materials, University of Groningen, Nijenborgh 4, 9747 AG Groningen, The Netherlands
[b] Macromolecular Chemistry & Biomaterials, Institute of Organic Chemistry III, University of Ulm, Albert-Einstein-Allee 11, D-89069 Ulm, Germany

ARTICLE INFO

Article history:
Received 28 November 2012
Accepted 13 February 2013
Available online 9 March 2013

Keywords:
GFP
Supercharged protein
Protein therapeutic
Fusion protein
Elastin-like polypeptide

ABSTRACT

One of the barriers to the development of protein therapeutics is effective delivery to mammalian cells. The proteins must maintain a careful balance of polar moieties to enable administration and distribution and hydrophobic character to minimize cell toxicity. Numerous strategies have been applied to this end, from appending additional cationic peptides to supercharging the protein itself, sometimes with limited success. Here we present a strategy that combines these methods, by equipping a protein with supercharged elastin-like polypeptide (ELP) tags. We monitored cellular uptake and cell viability for GFP reporter proteins outfitted with a range of ELP tags and demonstrated enhanced uptake that correlates with the number of positive charges, while maintaining remarkably low cytotoxicity and resistance to degradation in the cell. GFP uptake proceeded mainly through caveolae-mediated endocytosis and we observed GFP emission inside the cells over extended time (up to 48 h). Low toxicity combined with high molecular weights of the tag opens the way to simultaneously optimize cell uptake and pharmacokinetic parameters. Thus, cationic supercharged ELP tags show great potential to improve the therapeutic profile of protein drugs leading to more efficient and safer biotherapeutics.

1. Introduction

The application of proteins for therapy represents an emerging area and until now, around 180 protein drugs have been clinically approved including insulin, erythropoietin, interferons, and a variety of antibodies [1]. In contrast to small molecule drugs, therapeutic proteins are generally considered as biocompatible with higher specificity for their respective target. Until now, most protein therapeutics mainly address extracellular targets since exogenous proteins are typically not able to diffuse into cells [2]. The pharmacokinetic properties and bioavailability of drugs critically depend on their molecular weight and their ability to overcome cellular membranes. As a consequence, many promising drug candidates fail to advance in the clinic since they do not fulfill the structural requirements needed for cellular uptake; either they are too hydrophobic for administration and distribution or they are too polar or of too high molecular weight for passive cellular entry. The latter holds particularly true for protein therapeutics.

Over the past decade, a variety of reagents have been developed to allow the delivery of proteins into mammalian cells including lipid-linked compounds [3], nanoparticles [4], cationic peptides [5] and fusions to receptor ligands [6] like the protein transduction domains (PTDs) including the HIV-1 transactivator of transcription (Tat) peptide, oligoarginine, the Drosophila Antennapedia-derived penetratin peptide [7] and the (antiapoptotic) pentapeptides derived from the Bax binding domain of Ku70 [8]. These cell penetrating peptides (CPPs) can trigger the transfer of a cargo across the cell membrane into the cytoplasm. They are typically characterized by an amino acid composition that either contains a high abundance of positively charged amino acids such as lysine or arginine (polycationic) or exhibits an alternating pattern of polar/charged and non-polar, hydrophobic residues (amphiphilic). A typical polycationic peptide is poly-L-lysine (PLL), which has been used to efficiently deliver a range of biomolecules into cells including albumin and horseradish peroxidase [9]. Poly-L-arginine (PLA), a motif inspired by the naturally occurring CPPs, has been widely used both in vitro for the transfer of peptides [10] and in vivo for the delivery of proteins [11]. Arg7 and Arg9 have been used in vivo for the transfer of cyclosporine [12] and human catalase [13], respectively. Several experimental and theoretical studies were carried out to elucidate the mechanism for translocation of CPPs and to investigate the role of different positively charged amino acid residues [14,15]. However, it was also demonstrated that polycations can induce toxicity such as mitochondria-mediated apoptosis [16].

Rather than appending a polycationic peptide, another strategy for introducing positive charges is increasing the net charge of a

* Corresponding authors.
E-mail addresses: Tanja.Weil@uni-ulm.de (T. Weil), a.herrmann@rug.nl (A. Herrmann).
[1] Both authors have contributed equally.

0142-9612/$ – see front matter © 2013 Elsevier Ltd. All rights reserved.
http://dx.doi.org/10.1016/j.biomaterials.2013.02.038

polypeptide chain (henceforward called "supercharging"). This process enhances solubility and causes intermolecular repulsion even in the unfolded state, which in turn prevents aggregation [17]. Fusion to supercharged polypeptides enhances protein delivery in vitro and in vivo in a process that is clathrin- and energy-dependent, involving binding to anionic cell surface proteoglycans and endocytosis [2]. Using this approach, potent delivery vectors were realized by a "supercharged" variant of GFP [18], and by using a diverse class of naturally occurring supercharged human proteins [19]. Nevertheless, when rational supercharging was applied to other functional proteins like binding proteins (streptavidin) and enzymes (glutathione S-transferase) the modifications conferred increased thermal resistance but diminished function [20]. The "supercharging" of a protein by genetic mutation of surface-exposed amino acids requires, indeed, careful examination of the crystal structure to identify charged amino acid residues on the protein surface, mutation and shuffling of the gene sequence, and expression and screening for functional variants [2]. Moreover, it is not guaranteed that this process creates a functional variant with a certain desired surface charge.

We have previously reported the fabrication of unfolded supercharged polypeptides designed with elastin-like polypeptide (ELP) as the basic sequence [21]. These materials can be positively and negatively "supercharged" in a straightforward manner by introducing a lysine or glutamic acid residue at the second position of the repetitive pentapeptide sequence (GVGVP) [21]. This enables us to tune the overall charge of the protein by simply adjusting the length of the tag while obviating modification of the protein itself. At the same time, the lower charge density of the backbone in these ELP tags compared to other polycationic polymers such as polyarginine decreases cytotoxicity [21]. The suitability of neutral or weakly charged ELPs as materials for biomedical applications has been demonstrated in a number of publications. ELPs were employed as hydrogels for biosurface and tissue engineering [22] and for controlled release [23,24]. Furthermore, ELPs have been already used for delivery of drugs, peptides, proteins and DNA [24–26] and included in modified liposomes they enhance cellular uptake into tumor cells [27].

Thus positively supercharged tags based on ELP could be a suitable tool for facilitating cellular uptake of active proteins. In this contribution we tested whether positively "supercharged" ELP tags can serve as a platform for the delivery of proteins into mammalian cells, without altering their properties. Therefore, GFP was selected as a reporter protein and the cellular uptake of a functional variant of GFP fused to positively charged cationic ELP tags, with different numbers of charges (ranging from 9 to 72), was studied using an in vitro cell culture lung cell model (A549). Moreover, cell toxicity and cellular uptake mechanisms were investigated.

2. Materials and methods

2.1. Cloning and expression of GFP equipped with supercharged ELP tags

Monomers of the cationic and anionic ELP genes (K9 and E9) were ordered from Entelechon and were delivered in the pEN vector. Gene sequences and respective amino acid sequences of monomers are shown in Fig. S1. As the recognition sites of the restriction enzymes PflMI and BglI had to be preserved, one valine residue per ten pentapeptide repeats was incorporated instead of a lysine or glutamic acid residue. The ELP gene was excised from the pEN vector by digestion with EcoRI and HinDIII (Fermentas, St. Leon-Rot, Germany) and run on a 1% agarose gel (Sigma–Aldrich, St. Louis, MO) in TAE buffer (per 1 L, 108 g Tris base, 57.1 mL glacial acetic acid, 0.05 M EDTA, pH 8.0). The band containing the ELP gene was excised from the gel and purified using a spin column purification kit (QIAGEN). PUC19 (Fermentas, St. Leon-Rot, Germany) was digested with EcoRI and HinDIII and dephosphorylated. The vector was purified by agarose gel extraction following gel electrophoresis. The linearized pUC vector and the ELP-encoding gene were ligated and transformed into XL1-Blue cells (Stratagene, Cedar Creek, TX). For transformation, 20 μL of chemically competent *Escherichia coli* XL1-Blue cells were combined with 5 μL of the ligation mixture and further treated according to the manufacturer's protocol. Cells were spread on LB agar plates (for 1 L, 10 g Bacto™ tryptone, 5 g BBL™ yeast extract, 5 g NaCl, 15 g agar) supplemented with 100 μg/mL carbenicillin (Carl Roth, Karlsruhe, Germany), and incubated o/n at 37 °C. Colonies were picked and grown in 6 mL LB media (for 1 L, 10 g Bacto™ tryptone, 5 g BBL™ yeast extract, 5 g NaCl) (Becton, Dickinson and Co. Sparks, MD) supplemented with 100 μg/mL carbenicillin o/n, and plasmids were isolated using the Plasmid Miniprep kit (Fermentas, St. Leon-Rot, Germany). Positive clones were verified by plasmid digestion with EcoRI and HinDIII and the DNA sequence of putative inserts was further verified by DNA sequencing (SequenceXS, Leiden, The Netherlands). Gene oligomerization was performed as described by Chilkoti and co-workers (Fig. S2) [28].

The expression vector pET 25b(+) (Novagen Inc., San Diego, CA) was modified by cassette mutagenesis for incorporation of a unique SfiI recognition site as described before [21,28]. The modified pET 25b(+) vector (henceforward called pET-SfiI) was further digested with XbaI and NdeI (Fermentas, St. Leon-Rot, Germany), dephosphorylated and purified by a spin column purification kit. The GFP gene including the ribosomal binding site was excised from the pGFP vector (pGFP was a kind gift from Prof. D. Hilvert, Federal Institute of Technology, Zurich, Switzerland) by digestion with XbaI and SacI (Fermentas, St. Leon-Rot, Germany), and the excised gene (747 bp) was purified by agarose gel electrophoresis. A linker sequence that connects GFP and the SfiI restriction site was constructed in the following way: Oligonucleotides (Sigma–Aldrich, St. Louis, MO) linker_sens (cggtgtagtc ggtttagttc ccagaggaag tca) and linker_antisens (tatgacttcc tctgggaact aaaccgacta caccgagct), both 5′-phosphorylated, were mixed in equimolar ratios, incubated at 90 °C for 1 h and then cooled down stepwise to 20 °C for annealing (1 °C per 3 min). The resulting linker contained overhangs corresponding to a SacI and an NdeI restriction site, respectively. pET-SfiI, the insert containing GFP and the linker were ligated, yielding pET-GFP-SfiI. For insertion of ELP genes, pET-GFP-SfiI was digested with SfiI, dephosphorylated and purified using a microcentrifuge spin column kit. The respective ELP gene was excised from the pUC19 vector by digestion with PflMI and BglI, and the linearized vector and the insert containing the ELP gene were ligated, transformed into XL1-Blue cells, and screened as described above.

E. coli BLR (DE3) cells (Novagen) were transformed with the pET-SfiI expression vectors containing the respective ELP genes. For protein production, Terrific Broth medium (for 1 L, 12 g tryptone and 24 g yeast extract) enriched with phosphate buffer (for 1 L, 2.31 g potassium phosphate monobasic and 12.54 g potassium phosphate dibasic) (Merck KGaA, Darmstadt, Germany) and glycerol (4 mL per 1 L TB) (Merck) and supplemented with 100 μg/mL ampicillin (Roth), was inoculated with an o/n starter culture to an initial optical density at 600 nm (OD_{600}) of 0.1 and incubated at 37 °C with orbital agitation at 250 rpm until OD_{600} reached 0.7. Protein production was induced by a temperature shift to 30 °C. Cultures were then continued for additional 16 h post-induction. Cells were subsequently harvested by centrifugation (7000× *g*, 20 min, 4 °C), resuspended in lysis buffer (50 mM sodium phosphate buffer, pH 8.0, 300 mM NaCl, 20 mM imidazole (Carl Roth, Karlsruhe, Germany) for E variants or 10 mM Tris–HCl buffer, pH 8.0, 300 mM NaCl, 20 mM imidazole for K variants) to an OD_{600} of 100 and disrupted with a constant cell disrupter (Constant Systems Ltd., Northands, UK). Cell debris was removed by centrifugation (40,000× *g*, 90 min, 4 °C). Proteins were purified from the supernatant under native conditions by Ni-sepharose chromatography (GE Healthcare). Product-containing fractions were pooled and dialyzed against ultrapure water (>18 MΩ). K variants were further purified by affinity chromatography using a Heparin HP column (GE Healthcare), and E variants by anion exchange chromatography using a Q HP column (GE Healthcare). Protein-containing fractions were dialyzed extensively against ultrapure water (>18 MΩ). Purified proteins were frozen in liquid nitrogen, lyophilized and stored at −20 °C until further use.

2.2. Protein characterization

The concentrations of the purified ELPs were determined by measuring absorbance at 280 nm using a SpectraMax M2 (Molecular Devices, Sunnyvale, CA). Protein purity was determined by sodium dodecyl sulfate polyacrylamide gel electrophoresis (SDS-PAGE) on a 12% polyacrylamide gel (Bio-Rad Laboratories, Hercules, CA). Gels were stained with Coomassie staining solution (40% methanol, 10% glacial acetic acid, 1 g/L Brilliant Blue R250). Photographs of the gels were taken with a LAS-3000 Image Reader (Fuji Photo Film (Europe) GmbH, Dusseldorf, Germany).

Mass spectrometric analysis was performed using a 4800 MALDI-TOF/TOF Analyzer (Applied Biosystems, Foster City, CA, USA) in the linear positive mode. The protein samples were mixed 1:1 *v*/*v* with a recrystallized α-cyano-4-hydroxycinnamic acid matrix (10 mg/mL in 50% ACN and 0.1% TFA, LaserBio Labs). Mass spectra were analyzed and calibrated internally with the Data Explorer software, version 4.9 (Applied Biosystems, Foster City, CA, USA). Trypsinogen (M_w = 23,980), enolase (M_w = 46,672) (LaserBio Labs, Sophia-Antipolis, France) and bovine serum albumin (M_w = 66,431) (Carl Roth, Karlsruhe, Germany) were used as calibration standards.

Fluorescence spectra of GFP, GFP-K72 and GFP-E72 were recorded on a SpectraMax M2 (Molecular Devices, Sunnyvale, CA). GFP concentration in phosphate buffer solution (PBS) was determined by measuring absorbance at 488 nm. Volumes were adjusted with PBS until absorbance at 488 nm was between 0.82 and 0.85. Samples were diluted ten times in PBS for fluorescence measurements. Fluorescence

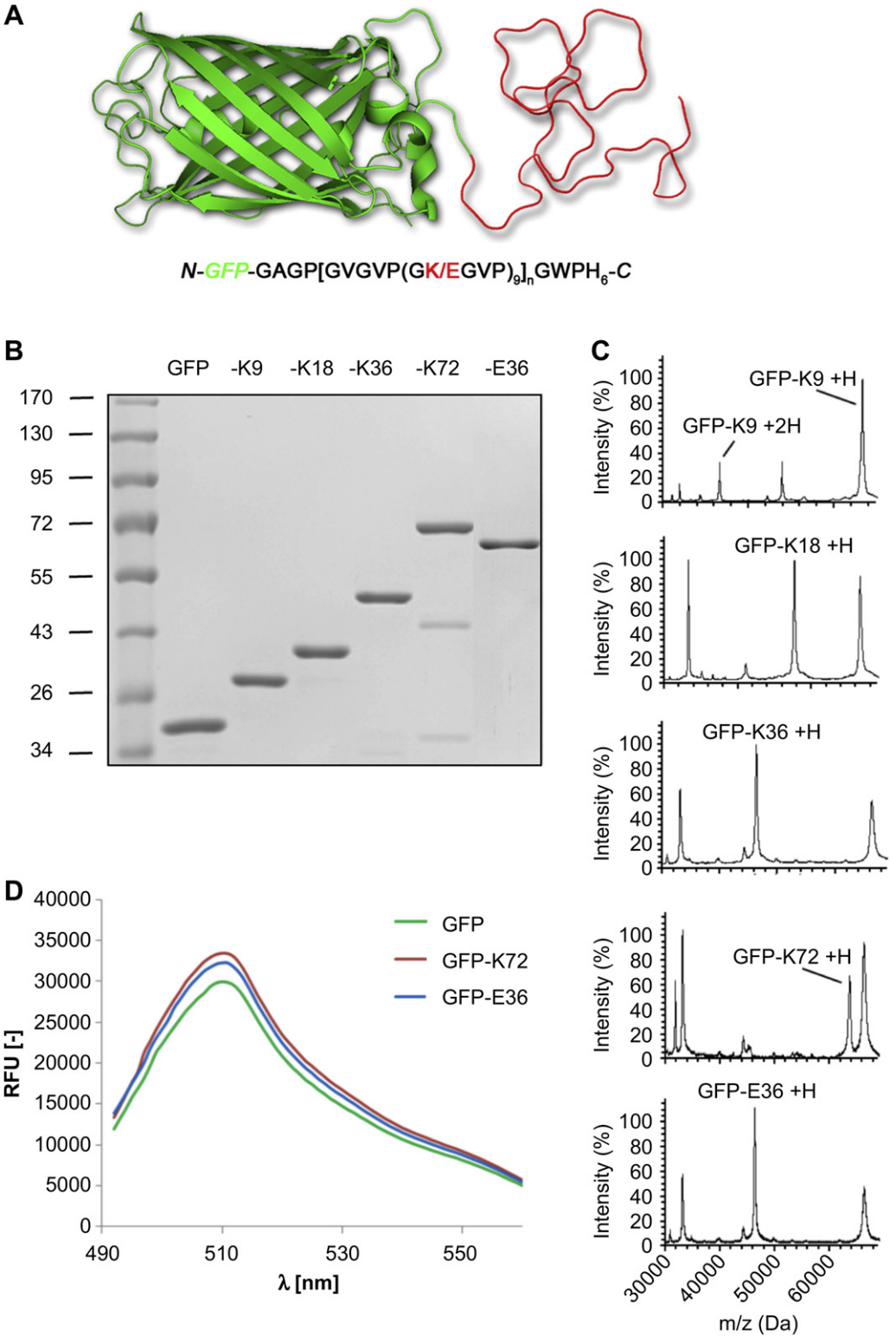

Fig. 1. Characterization of GFP fusion variants of supercharged elastin-like proteins (A) schematic representation of GFP–ELP fusion proteins. GFP (green) shows the characteristic beta-barrel structure, whereas the ELP is presented as an extended coil (red) without exhibiting a defined secondary or tertiary structure. (B) GFP–ELP fusion proteins separated on a 12% SDS-PAGE gel and stained with Coomassie brilliant blue R250. (C) MALDI-TOF mass spectra of supercharged elastin-like proteins fused to GFP. From top to bottom: GFP-K9; GFP-K18; GFP-K36; GFP-K72; GFP-E36. Internal standards are enolase (GFP-K18), bovine serum albumin (GFP-E36, GFP-K36, GFP-K72) and trypsinogen (GFP-K9). (D) Fluorescence spectra of GFP and GFP–ELP variants GFP-K72 and GFP-E72 upon excitation at 488 nm. Spectra are averages of three measurements.

spectra were recorded upon excitation at 488 nm. Measurements were carried out in triplicates and average fluorescence values were corrected for differences in absorbance according to RFUcorr = RFUmeas···0.84/abs488, with RFUcorr being the corrected relative fluorescence unit (RFU), RFUmeas the measured RFU, and abs488 the measured absorbance at 488 nm of the ten times concentrated solution.

2.3. Cell culture

A549 cells, a human alveolar basal epithelial carcinoma cell line, were obtained from DSMZ (German Collection of Microorganisms and Cell Cultures, Braunschweig). Cells were cultured in high-glucose DMEM (Dulbecco's Modified Eagle Medium) supplemented with 10% fetal bovine serum (FBS), 100 U/mL penicillin, 0.1 mg/mL streptomycin, and 0.1 mM non-essential amino acids at 37 °C in a humidified 5% CO_2 incubator.

2.4. Quantification of cell uptake

A549 cells were seeded in a 96-well microplate at a concentration of 80,000 cells/well. After overnight culture, the cells were incubated with 1 μM of different GFP variants in 100 μL fresh medium for 24 h. The cells were then washed three times with ice-cold PBS to remove the non-internalized samples and lysed with 100 μL of lysis buffer (50 mM Tris, 0.8% Triton, 0.2% SDS, pH 7.4) [29]. Cell-associated GFP was determined by measuring the fluorescence of the lysate using a TECAN Infinite M1000 microplate reader (Ex 488 nm and Em 510 nm) [30]. All data were collected in triplicate and two independent experiments were performed to calculate the average cellular uptake.

2.5. Confocal microscopy

A549 cells were plated in a Coverglass Lab-Tek 8-well chamber and incubated overnight to allow adhesion. The next day, fresh medium with 1 μM of GFP variants were added to the cells and further incubated for 24 h. Before imaging, cells were washed with PBS buffer three times and then the cell membrane was stained with CellMask™ Deep Red plasma membrane stain for 5 min. Imaging was performed using an LSM 710 laser scanning confocal microscope system (Zeiss, Germany) coupled to an XL-LSM 710 S incubator and equipped with a 63× oil immersion objective. The GFP variants were excited with a 488 nm argon laser and detected after a 493 nm–599 nm emission filter. The membrane stain was excited with a HeNe laser (emission wavelength 633 nm) and detected after a 647 nm–759 nm emission filter. During the experiments, the samples were mounted on a temperature-controlled microscope stage, which kept the cells at 37 °C.

2.6. Cytotoxicity assay

Eight thousand A549 cells per well were plated onto a white 96-well plate and incubated overnight to allow attachment. The wells were 70–80% confluent on the day of the experiment. The cells were treated with 1, 5 and 10 μM GFP variants or 1 μM doxorubicin as a positive control and incubated for another 24 h. Blank cells without treatment were used to obtain 100% cell viability. After treatment, the CellTiter Glo™ (Promega) cell viability assay kit was used to quantify the viability of the cells in each well according to the manufacturer's instructions.

2.7. Exploring uptake pathways using different endocytosis inhibitors

The cells were pre-incubated for 30 min with the following inhibitors: (i) 10 μg/mL and 1 μg/mL of chlorpromazine to inhibit clathrin-mediated endocytosis, (ii) 1 μg/mL and 0.1 μg/mL of filipin to inhibit caveolae-mediated endocytosis, (iii) 40 μM and 5 μM of amiloride to inhibit macropinocytosis. (All inhibitors were obtained from Sigma–Aldrich.) Each concentration of the inhibitors was chosen based on previous studies [31–33] and it was also observed that at these concentrations, greater than 80% of the cells were viable by Cell-Titer Glo™ (Promega) cell viability assay. Subsequently, the different GFP variants (1 μM) were added to the supernatant containing the inhibitors and the cells were incubated at 37 °C for 2 h. The cell uptake was then quantified using fluorescence as mentioned above. Under the same inhibition conditions, cell uptake of endocytosis markers (Alex-488 transferrin as clathrin-mediated endocytosis marker [33], BODIPY–lactosylceramide as caveolae-mediated endocytosis marker [34], FITC–dextran as macropinocytosis marker [31]) were inhibited by >80%. The effect of temperature block was studied by pre-incubating the cells at 4 °C for 30 min and treatment with GFP variants (1 μM) for 2 h at 4 °C.

2.8. Statistical analysis

Statistical significance of the observed differences was evaluated by a one-way ANOVA test followed by Dunnett's test. A value of $P < 0.05$ was considered significant.

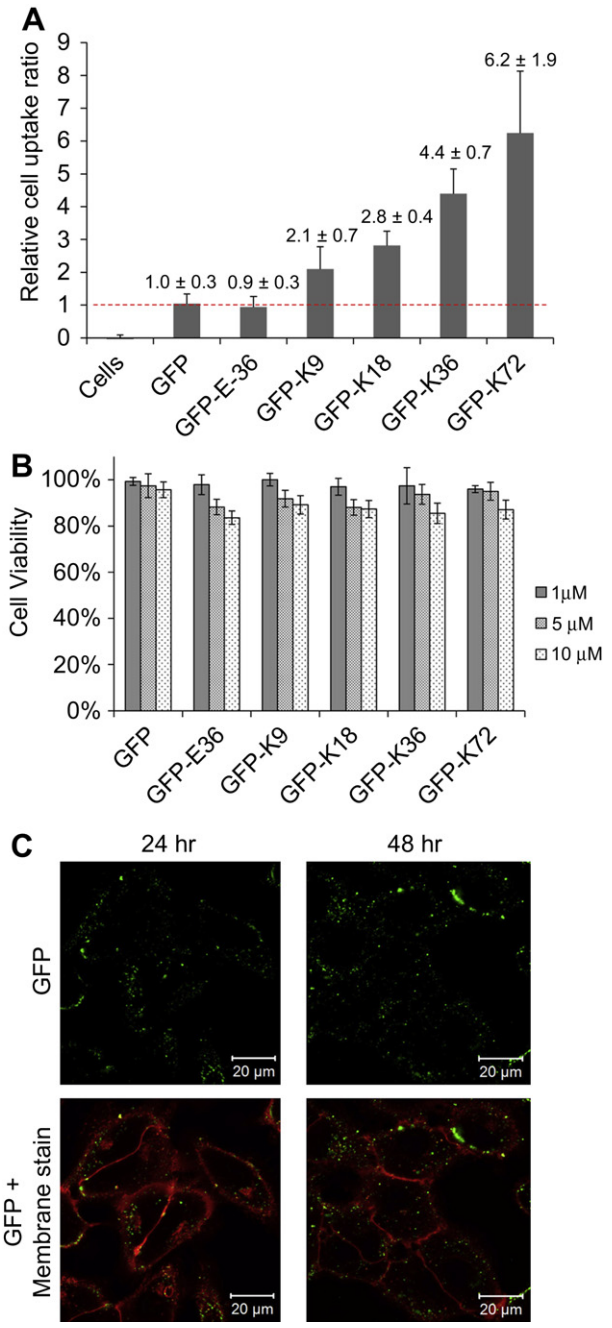

Fig. 2. (A) The relative cell uptake ratio has been calculated compared to native GFP uptake, which has been set to 1. Each column presents average value of 6 measurements from two independent experiments. The error bar presents the standard deviation. (B) The cell viability of each sample has been calculated. Cells in blank samples are considered as 100% viable. Each column presents the average value of 3 independent measurements. The error bar presents the standard deviation. (C) Confocal micrograph of A549 cells incubated with 1 μM of GFP-K72 at 24 and 48 h.

3. Results and discussion

3.1. Preparation and characterization of supercharged GFP–ELP fusion proteins

Genes encoding for cationic and anionic supercharged protein tags of different lengths were generated by recursive directional ligation of the ELP monomer gene (Fig. S1) [27]. An ELP monomer consists of 10 repeating units of the pentapeptide sequence GXGVP, with G denoting the amino acid glycine, V valine, P proline and X

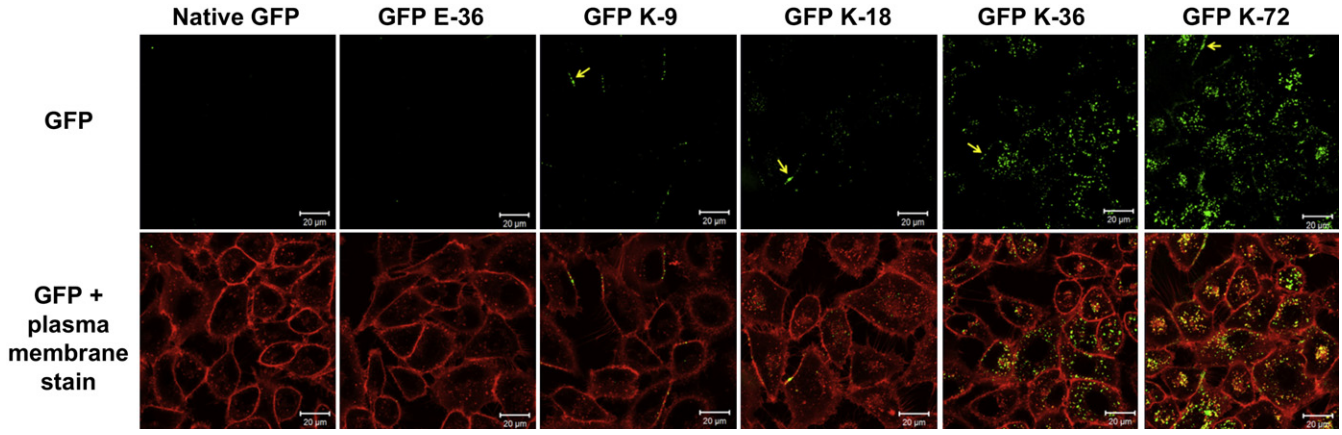

Fig. 3. Confocal microscope imaging of A549 cells incubated with 1 μM GFP derivatives for 24 h. Arrows indicate membrane aggregation.

either glutamic acid (E), lysine (K) or V. To preserve the restriction site that is needed for multimerization, V is inserted at position X in one out of ten pentapeptide repeats (Fig. 1A). After multimerization, the ELP genes were cloned into a bacterial expression vector containing the GFP gene and a sequence encoding a hexahistidine tag for affinity purification. GFP encodes GFP plus, a variant of enhanced green fluorescent protein, hereafter named GFP (Fig. S3). We realized fusion variants of GFP with supercharged protein tags containing between 9 and 72 positive charges and one with 36 negative charges. The exact sequence composition for the positive variants were N–*GFP*–GAGP[GVGVP(G**K**GVP)$_9$]$_n$GWPH$_6$–C (with *n* ranging from 1 to 8) while the negatively charged fusion construct exhibited the sequence N–*GFP*–GAGP[GVGVP(G**E**GVP)$_9$]$_4$GWPH$_6$–C (Fig. 1A). In this work, GFP-E*x* and GFP-K*x* denote GFP with anionic and cationic tags, respectively, with *x* displaying the number of charged residues in the tag. All variants were successfully expressed in and purified from *E. coli* cells. Typically, a 50 mL culture yielded up to 1 mg of purified protein. Molecular weight and purity were confirmed by gel electrophoresis (Fig. 1B) and mass spectrometry (Fig. 1C). Values determined by mass spectrometry were in good agreement with the masses that were calculated based on the amino acid sequence (Table S1). For all variants, GFP was found to be fluorescent. Fluorescence spectra were recorded for GFP, GFP-K72 and GFP-E36 (the longest charged chains we realized) (Fig. 1D). GFP fluorescence was not decreased or shifted, indicating that even the long positively and negatively charged tags did not interfere with GFP function. A schematic representation of GFP–ELP fusion proteins (Fig. 1A) shows GFP (green) drawn with its characteristic beta-barrel structure, whereas the ELP is presented as an extended coil (red) without exhibiting a defined secondary or tertiary structure, as was demonstrated previously [21].

3.2. Cellular uptake of supercharged GFP–ELP fusion proteins

The influence of these tags on the in vitro cellular uptake of the GFP fusion variants was studied with a representative mammalian cell line (A549). The uptake of the various GFP species was quantified by fluorimetry [29,35] and a charge dependent cellular uptake was clearly observed. The fusion of the negatively charged elastin tag with 36 charges to GFP (GFP-E36) had no influence on internalization compared to the unmodified GFP (Fig. 2A). In contrast, pronounced cellular uptake for all positively supercharged GFP variants compared to the control protein was detected. Notably, the internalization increased with increasing the number of positive charges within the supercharged tags. GFP-K9 uptake doubled while GFP-K72 was incorporated six times more efficiently than pristine GFP (Fig. 2A). Previously, neutral elastin-like polypeptides were employed as delivery vehicles for small therapeutic peptides [36] and proteins [37]. However, with those systems uptake into cancerous tissue and cells was mediated by exploiting their thermoresponsive properties and fused CCP motifs, respectively. Both features are not present in our supercharged ELP variants systems indicating that we pursue a new paradigm for cellular uptake regarding ELPs. In the context of charge dependent uptake with supercharged ELP tags significant differences to supercharged GFP where lysine and arginine residues are present at the surface of the protein were also revealed. With this supercharged GFP variants a high-potency uptake regime was observed at a theoretical positive net charge of 22 with no significant improvement of uptake when the number of charges is further increased [38]. In contrast, we detected a delivery potency increase even up to 72 theoretical net charges.

3.3. Intracellular localization

In the next step the intracellular localization of the GFP derivatives was assessed using confocal fluorescence microscopy (Fig. 3). When A549 cells were incubated with GFP and GFP-E36 for 24 h, no significant fluorescence signal associated with the cells was observed. However, when the cells were treated with the GFP-K9 sample, GFP fluorescence was mainly detected on the cell membrane. In comparison, GFP-K18 was already observed inside A549 cells, although some of the protein was still present as aggregates on the cellular membrane. Such an aggregation behavior has been reported previously for other positively charged macromolecules as well [39], indicating that a strong interaction between the polycationic samples and the negatively charged cell membrane represents a first, essential step for interaction. Only GFP-K36 and GFP-K72 revealed significant internalization and in particular, GFP-K72 generated the strongest emission signal recorded inside A549 cells. Interestingly, we detected the signal of GFP-K72 even over an extended period of time up to 48 h (Fig. 2C). These observations are in good agreement with the quantitative uptake data obtained by fluorimetry and prove efficient protein uptake mediated by positively supercharged ELP tags bearing 36 and 72 positive charges. Moreover, in the presence of serum, no aggregation with serum proteins was observed under the microscope for any GFP–ELP fusion protein, which is essential for any application in vivo.

3.4. Cytotoxicity study

Cytotoxicity of all the GFP variants was assessed under the same conditions as used for the cell uptake experiments. The assay is based on the quantification of ATP, an indicator of metabolically

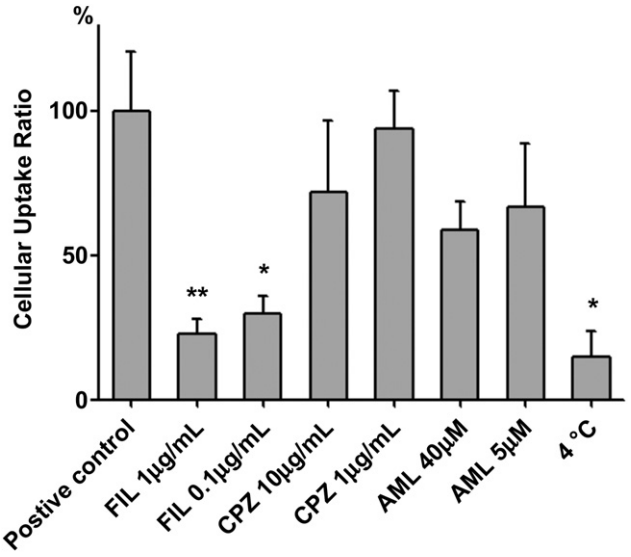

Fig. 4. Effects of inhibitors on internalization of GFP-K72. Cells were pretreated under 4 °C or with filipin (FIL), chlorpromazine (CPZ) and amiloride (AML) and subsequently incubated with GFP-K72 for 2 h (for the details see Materials and methods). The fluorescence from GFP-K72 was measured by microplate reader. The fluorescence intensity in positive control cells was set as 100%. Mean values and standard deviation were obtained from triplicate experiments. One-way ANOVA test followed by Dunnett's test was carried out to determine the statistical significance of the data ($^{*}P < 0.05$; $^{**}P < 0.01$).

active cells, *via* the generation of a luminescent signal. The amount of ATP is directly proportional to the number of cells present in culture. As shown in Fig. 2B, cells showed no loss in cell viability when incubated for 24 h with GFP-derivates below a concentration of 1 μM, and even for higher concentrations of up to 10 μM no effect of the ELP length on cytotoxicity was observed. In comparison, positively charged polymers such as poly-L-lysine and poly(-ethylene)imine very often display significant cytotoxicities, revealing that the charge density plays an important role [40]. Even a short polyarginine tag showed an EC50 value of about 9 μM in A549 cells [41]. Systematic studies suggested that aggregation as well as disruption of membrane integrity are reasons for cytotoxicity [42] Strategies such as masking of positive charges have been applied to decrease cytotoxicity [43,44]. However, fine-tuning the number and density of positive charges for cell uptake is not always trivial. In contrast, polycationic proteins, such as supercharged albumins, were applied in comparatively high quantities before cell toxicity was observed which has been attributed to their low charge density dissipated within a larger volume [45,46]. Therefore, the cationic ELP tags and in particular GFP-K72 offers an increased molecular weight and hydrodynamic volume, lower charge densities and no increase in cytotoxicity compared with the conventional polycationic tags, such as the polyarginine tag, which display high density of positive charges. The increase of molecular weight induced by the tag could potentially induce an enhanced blood circulation of the respective protein or an accumulation in tumor tissue *via* the EPR-effect, which are both known to be size dependent. These aspects will be addressed in future studies.

3.5. Cell uptake pathway

Several mechanisms are known by which macromolecules can enter cells, including energy-dependent mechanisms, such as endocytosis or macropinocytosis as well as other non-energy dependent mechanisms [47]. Investigation of the cell uptake pathway represents an essential step to understand the intracellular fate of a molecule and assess its intracellular functions. We have studied the uptake pathway of GFP-K72 tagged with supercharged ELP in A549 cells. GFP-K72 was selected because it displayed the most significant cell uptake. The energy dependency of cell uptake was investigated by incubation at 4 °C and 37 °C. Incubation at the lower temperature resulted in a significant, about 85% reduction of the entire cell uptake (Fig. 4), indicating that GFP-K72 uptake mainly proceeded through energy-dependent pathways. However 15% of cell uptake remained at 4 °C indicating that energy-independent direct translocation may play a minor role. Different endocytosis inhibitors were then applied to determine the specific energy-dependent endocytic pathway by which GFP-K72 is internalized. Cells were pre-incubated with inhibitors for 30 min followed by incubating with 1 μM of GFP-K72 for 2 h. The cell uptake was assayed by a fluorescence microplate reader as described above. We observed the most significant suppression of GFP-K72 uptake with Filipin (FIL), which is known to inhibit caveolae-mediated endocytosis [48]. After the application of only 0.1 μg/mL FIL a >70% reduction of cellular uptake was observed. In comparison, only insignificant effects were detected upon treatment with the clathrin-mediated endocytosis inhibitor chlorpromazine hydrochloride (CPMZ) [49] or the macropinocytosis inhibitor amiloride (Fig. 4). These observations suggest that cell uptake of GFP-K72 mainly proceeds through caveolae-mediated endocytic pathways and that clathrin-mediated endocytosis and macropinocytosis only play a minor role. It has been reported previously that particles internalized *via* clathrin-mediated endocytosis are delivered to the lysosomes whereas uptake *via* caveolae allows escaping lysosomal pathways and trafficking to the endoplasmic reticulum of the cell [50,51]. In view of the delivery of therapeutic proteins, it is an attractive feature that ELP supercharged tags facilitate cell uptake *via* the caveolae-mediated pathway, as this should minimize protein degradation in lysosomes. This feature is supported by the fact that the fluorescence of the GFP variants was observed inside the cells even after 48 h of incubation.

In comparison, some short CPPs were found to enter cells *via* macropinocytosis [52,53] and folded supercharged proteins including GFP were taken up predominantly by clathrin-dependent endocytosis [38]. In the context of ELP uptake, previously neutral variants were reported to penetrate cells *via* a caveolae-independent endocytic mechanism [26]. These uptake mechanisms are in stark contrast to the internalization of our supercharged ELP fusions indicating how the charge, the molecular weight and the folding state of the tag are important for determining uptake pathways. In general, the cellular uptake pathways studied in the literature are difficult to compare. Factors such as the concentration of peptides, the ionic strength of the medium [54], the nature of the cell lines and the presence and type of cargo [55,56] have a significant influence on the uptake mechanism.

4. Conclusions

In summary, we have shown the expression of the fluorescent reporter protein GFP bearing rationally designed ELP supercharged tags of varying lengths with an unprecedented number of charges. Furthermore, we observed that their cellular uptake strongly depends on the number of positive charges present in the tag. The most positive charged protein, GFP-K72 (theoretical positive net charge: 72), exhibited a roughly six fold increase in uptake compared to unmodified GFP, and indeed a significant amount of GFP was detected inside the cells even after 48 h. Investigating the mechanism, we showed that cell uptake proceeds primarily *via* caveolae-mediated endocytosis. Finally, we believe that the facile introduction of supercharged elastin-like tags by genetic engineering has a high potential to improve cellular uptake and critical

pharmacokinetic parameters. Therefore, such tags complement existing poly-L-arginine or poly-L-lysine sequences as well as folded supercharged proteins. Due to the growing importance of protein therapeutics the discovery of tags improving their delivery is of high significance to allow a better translation into preclinical and clinical research.

Acknowledgment

T.W. thanks the German Research Foundation (DFG) under grant P3246029 and the Volkswagenstiftung (Aktenzeichen 86 366) for their financial support of this work.

A.H. acknowledges financial support from the EU (ERC starting grant NUCLEOPOLY), from NWO (VICI grant, ECHO grant) and from the Zernike Institute for Advanced Materials.

Appendix A. Supplementary data

Supplementary data related to this article can be found at http://dx.doi.org/10.1016/j.biomaterials.2013.02.038.

References

[1] Overington JP, Al-Lazikani B, Hopkins AL. How many drug targets are there? Nat Rev Drug Discov 2006;5:993–6.
[2] Thompson DB, Cronican JJ, Liu DR. Engineering and identifying supercharged proteins for macromolecule delivery into mammalian cells. Meth Enzymol 2012;503:293–319.
[3] Zelphati O, Wang Y, Kitada S, Reed JC, Felgner PL, Corbeil J. Intracellular delivery of proteins with a new lipid-mediated delivery system. J Biol Chem 2001;276:35103–10.
[4] Hasadsri L, Kreuter J, Hattori H, Iwasaki T, George JM. Functional protein delivery into neurons using polymeric nanoparticles. J Biol Chem 2009;284:6972–81.
[5] Holm T, Johansson H, Lundberg P, Pooga M, Lindgren M, Langel Ü. Studying the uptake of cell-penetrating peptides. Nat Protoc 2006;1:1001–5.
[6] Rizk SS, Luchniak A, Uysal S, Brawley CM, Rock RS, Kossiakoff AA. An engineered substance P variant for receptor-mediated delivery of synthetic antibodies into tumor cells. Proc Natl Acad Sci U S A 2009;106:11011–5.
[7] Heitz F, Morris MC, Divita G. Twenty years of cell-penetrating peptides: from molecular mechanisms to therapeutics. Br J Pharmacol 2009;157:195–206.
[8] Gomez JA, Gama V, Yoshida T, Sun W, Hayes P, Leskov K, et al. Bax-inhibiting peptides derived from Ku70 and cell-penetrating pentapeptides. Biochem Soc Trans 2007;35:797–801.
[9] Shen WC, Ryser HJ. Conjugation of poly-L-lysine to albumin and horseradish peroxidase: a novel method of enhancing the cellular uptake of proteins. Proc Natl Acad Sci U S A 1978;75:1872–6.
[10] Chen L, Wright LR, Chen CH, Oliver SF, Wender PA, Mochly-Rosen D. Molecular transporters for peptides: delivery of a cardioprotective epsilonPKC agonist peptide into cells and intact ischemic heart using a transport system, R(7). Chem Biol 2001;8:1123–9.
[11] Chen L, Hahn H, Wu G, Chen CH, Liron T, Schechtman D, et al. Opposing cardioprotective actions and parallel hypertrophic effects of delta PKC and epsilon PKC. Proc Natl Acad Sci U S A 2001;98:11114–9.
[12] Rothbard JB, Garlington S, Lin Q, Kirschberg T, Kreider E, McGrane PL, et al. Conjugation of arginine oligomers to cyclosporin A facilitates topical delivery and inhibition of inflammation. Nat Med 2000;6:1253–7.
[13] Jin LH, Bahn JH, Eum WS, Kwon HY, Jang SH, Han KH, et al. Transduction of human catalase mediated by an HIV-1 TAT protein basic domain and arginine-rich peptides into mammalian cells. Free Radic Biol Med 2001;31:1509–19.
[14] Su Y, Doherty T, Waring AJ, Ruchala P, Hong M. Roles of arginine and lysine residues in the translocation of a cell-penetrating peptide from (13)C, (31)P, and (19)F solid-state NMR. Biochemistry 2009;48:4587–95.
[15] Su Y, Li S, Hong M. Cationic membrane peptides: atomic-level insight of structure-activity relationships from solid-state NMR. Amino Acids 2012;44:821–33.
[16] Hudecz F, Gaál D, Kurucz I, Lányi Á, Kovács AL, Mezö G, et al. Carrier design: cytotoxicity and immunogenicity of synthetic branched polypeptides with poly(L-lysine) backbone. J Control Release 1992;19:231–43.
[17] Simeonov P, Berger-Hoffmann R, Hoffmann R, Sträter N, Zuchner T. Surface supercharged human enteropeptidase light chain shows improved solubility and refolding yield. Protein Eng Des Sel 2011;24:261–8.
[18] Cronican JJ, Thompson DB, Beier KT, McNaughton BR, Cepko CL, Liu DR. Potent delivery of functional proteins into mammalian cells in vitro and in vivo using a supercharged protein. ACS Chem Biol 2010;5:747–52.
[19] Cronican JJ, Beier KT, Davis TN, Tseng J-C, Li W, Thompson DB, et al. A class of human proteins that deliver functional proteins into mammalian cells in vitro and in vivo. Chem Biol 2011;18:833–8.
[20] Lawrence MS, Phillips KJ, Liu DR. Supercharging proteins can impart unusual resilience. J Am Chem Soc 2007;129:10110–2.
[21] Kolbe A, del Mercato LL, Abbasi AZ, Rivera Gil P, Gorzini SJ, Huibers WHC, et al. De novo design of supercharged, unfolded protein polymers, and their assembly into supramolecular aggregates. Macromol Rapid Commun 2010;32:186–90.
[22] Nettles DL, Chilkoti A, Setton LA. Applications of elastin-like polypeptides in tissue engineering. Adv Drug Deliv Rev 2010;62:1479–85.
[23] Megeed Z, Haider M, Li D, O'Malley BW, Cappello J, Ghandehari H. In vitro and in vivo evaluation of recombinant silk-elastin like hydrogels for cancer gene therapy. J Control Release 2004;94:433–45.
[24] Dandu R, Ghandehari H. Delivery of bioactive agents from recombinant polymers. Prog Polym Sci 2007;32:1008–30.
[25] MacEwan SR, Chilkoti A. Elastin-like polypeptides: biomedical applications of tunable biopolymers. Biopolymers 2010;94:60–77.
[26] Bidwell GL, Raucher D. Cell penetrating elastin-like polypeptides for therapeutic peptide delivery. Adv Drug Deliv Rev 2010;62:1486–96.
[27] Na K, Lee SA, Jung SH, Hyun J, Shin BC. Elastin-like polypeptide modified liposomes for enhancing cellular uptake into tumor cells. Colloids Surf B 2012;91:130–6.
[28] Meyer D, Chilkoti A. Genetically encoded synthesis of protein-based polymers with precisely specified molecular weight and sequence by recursive directional ligation: examples from the elastin-like polypeptide system. Biomacromolecules 2002;3:357–67.
[29] Ren Y, Wong SM, Lim L-Y. Folic acid-conjugated protein cages of a plant virus: a novel delivery platform for doxorubicin. Bioconjug Chem 2007;18:836–43.
[30] Liu SQ, Tong YW, Yang Y-Y. Incorporation and in vitro release of doxorubicin in thermally sensitive micelles made from poly(N-isopropylacrylamide-co-N, N-dimethylacrylamide)-b-poly(D, L-lactide-co-glycolide) with varying compositions. Biomaterials 2005;26:5064–74.
[31] Lacerda L, Russier J, Pastorin G, Herrero MA, Venturelli E, Dumortier H, et al. Translocation mechanisms of chemically functionalised carbon nanotubes across plasma membranes. Biomaterials 2012;33:3334–43.
[32] Zelikin AN, Breheney K, Robert R, Tjipto E, Wark K. Cytotoxicity and internalization of polymer hydrogel capsules by mammalian cells. Biomacromolecules 2010;11:2123–9.
[33] Perumal OP, Inapagolla R, Kannan S, Kannan RM. The effect of surface functionality on cellular trafficking of dendrimers. Biomaterials 2008;29:3469–76.
[34] Puri V, Watanabe R, Singh RD, Dominguez M, Brown JC, Wheatley CL, et al. Clathrin-dependent and -independent internalization of plasma membrane sphingolipids initiates two Golgi targeting pathways. J Cell Biol 2001;154:535–47.
[35] Lin R, Shi Ng L, Wang C-H. In vitro study of anticancer drug doxorubicin in PLGA-based microparticles. Biomaterials 2005;26:4476–85.
[36] Massodi I, Moktan S, Rawat A, Bidwell GL, Raucher D. Inhibition of ovarian cancer cell proliferation by a cell cycle inhibitory peptide fused to a thermally responsive polypeptide carrier. Int J Cancer 2010;126:533–44.
[37] Shamji MF, Chen J, Friedman AH, Richardson WJ, Chilkoti A, Setton LA. Synthesis and characterization of a thermally-responsive tumor necrosis factor antagonist. J Control Release 2008;129:179–86.
[38] Thompson DB, Villaseñor R, Dorr BM, Zerial M, Liu DR. Cellular uptake mechanisms and endosomal trafficking of supercharged proteins. Chem Biol 2012;19:831–43.
[39] Godbey WT, Wu KK, Mikos AG. Tracking the intracellular path of poly (ethylenimine)/DNA complexes for gene delivery. Proc Natl Acad Sci U S A 1999;96:5177–81.
[40] Beyerle A, Merkel O, Stoeger T, Kissel T. PEGylation affects cytotoxicity and cell-compatibility of poly(ethylene imine) for lung application: structure–function relationships. Toxicol Appl Pharmacol 2010;242:146–54.
[41] Jones SW, Christison R, Bundell K, Voyce CJ, Brockbank SMV, Newham P, et al. Characterisation of cell-penetrating peptide-mediated peptide delivery. Br J Pharmacol 2005;145:1093–102.
[42] Leroueil PR, Hong S, Mecke A, Baker JR, Orr BG, Banaszak Holl MM. Nanoparticle interaction with biological membranes: does nanotechnology present a Janus face? Acc Chem Res 2007;40:335–42.
[43] Choi YH, Liu F, Park JS, Kim SW. Lactose-poly(ethylene glycol)-grafted poly-L-lysine as hepatoma cell-targeted gene carrier. Bioconjug Chem 1998;9:708–18.
[44] Lee H, Jeong JH, Park TG. PEG grafted polylysine with fusogenic peptide for gene delivery: high transfection efficiency with low cytotoxicity. J Control Release 2002;79:283–91.
[45] Choksakulnimitr S, Masuda S, Tokuda H, Takakura Y, Hashida M. In vitro cytotoxicity of macromolecules in different cell culture systems. J Control Release 1995;34:233–41.
[46] Eisele K, Gropeanu RA, Zehendner CM, Rouhanipour A, Ramanathan A, Mihov G, et al. Fine-tuning DNA/albumin polyelectrolyte interactions to produce the efficient transfection agent cBSA-147. Biomaterials 2010;31:8789–801.
[47] Canton I, Battaglia G. Endocytosis at the nanoscale. Chem Soc Rev 2012;41:2718–39.
[48] Schnitzer JE, Oh P, Pinney E, Allard J. Filipin-sensitive caveolae-mediated transport in endothelium: reduced transcytosis, scavenger endocytosis, and capillary permeability of select macromolecules. J Cell Biol 1994;127:1217–32.
[49] Wang LH, Rothberg KG, Anderson RG. Mis-assembly of clathrin lattices on endosomes reveals a regulatory switch for coated pit formation. J Cell Biol 1993;123:1107–17.

[50] Rejman J, Oberle V, Zuhorn IS, Hoekstra D. Size-dependent internalization of particles via the pathways of clathrin- and caveolae-mediated endocytosis. Biochem J 2004;377:159–69.
[51] Shin JS, Abraham SN. Caveolae as portals of entry for microbes. Microb Infect 2001;3:755–61.
[52] Wadia JS, Stan RV, Dowdy SF. Transducible TAT-HA fusogenic peptide enhances escape of TAT-fusion proteins after lipid raft macropinocytosis. Nat Med 2004;10:310–5.
[53] Nakase I, Tadokoro A, Kawabata N, Takeuchi T, Katoh H, Hiramoto K, et al. Interaction of arginine-rich peptides with membrane-associated proteoglycans is crucial for induction of actin organization and macropinocytosis. Biochemistry 2007;46:492–501.
[54] Guterstam P, Madani F, Hirose H, Takeuchi T, Futaki S, Andaloussi El S, et al. Elucidating cell-penetrating peptide mechanisms of action for membrane interaction, cellular uptake, and translocation utilizing the hydrophobic counter-anion pyrenebutyrate. Biochim Biophys Acta 2009;1788:2509–17.
[55] Säälik P, Elmquist A, Hansen M, Padari K, Saar K, Viht K, et al. Protein cargo delivery properties of cell-penetrating peptides. A comparative study. Bioconjug Chem 2004;15:1246–53.
[56] Richard JP, Melikov K, Brooks H, Prevot P, Lebleu B, Chernomordik LV. Cellular uptake of unconjugated TAT peptide involves clathrin-dependent endocytosis and heparan sulfate receptors. J Biol Chem 2005;280:15300–6.